HIGH RESOLUTION NUMERICAL MODELLING OF TSUNAMI INUNDATION USING QUADTREE METHOD AND GPU ACCELERATION

SHUANG GAO
BMT, Brisbane, Australia. shuang.gao@bmtglobal.com

GREG COLLECUTT
BMT, Brisbane, Australia. greg.collecutt@bmtglobal.com

WILLIAM J. SYME
BMT, Brisbane, Australia. bill.syme@bmtglobal.com

PHILIP RYAN
BMT, Brisbane, Australia. phillip.ryan@bmtglobal.com

ABSTRACT

This study adapted the quadtree mesh in TUFLOW's HPC 2D Shallow Water Equation (SWE) solver and investigated its feasibility of modelling tsunami inundation in coastal urban environments. The spatial mesh resolution was increased in the onshore urbanised area to reproduce the wave propagation at street scale, whereas a larger mesh size was used in offshore areas in order to reduce the total number of computational mesh elements. A 'Sub-Grid-Sampling' approach was also applied to mitigate the numerical head loss along wet/dry boundaries that are misaligned with the mesh. Model benchmark testing was conducted against a 1:50 scale flume experiment of the town Seaside, Oregon. The benchmarking results showed excellent agreement with the measured data and proved the numerical efficiency of the proposed quadtree mesh model. Furthermore, the combination of quadtree mesh and SGS approach offers great potential as an easy to construct, fast, high-resolution numerical tool to support tsunami hazard planning.

Keywords: Tsunami, numerical modelling, quadtree, GPU acceleration, TUFLOW

1. INTRODUCTION

The techniques of tsunami inundation modelling have advanced significantly in the past decades, and numerical simulation has become an essential part of tsunami hazard planning in coastal urban environments. Traditionally, numerical models had low spatial resolution and the flow resistance caused by obstacles (macro-roughness) was modelled by increasing bed roughness and/or adjusting cell porosity. This approach may slow tsunami propagation speed in an urbanised area compared to a less obstructive land-use but cannot provide guidance on the hazards at street scale. Flume experiments (Rueben et al., 2011, Park et al. 2013) and visual data obtained during past tsunami events have shown that destructive fast-moving currents form in open flow paths as the tsunami propagates through a densely urbanised area, and thus, a street-level spatial resolution is required to support effective evacuation planning and tsunami risk management.

Akoh et al. (2017) applied high resolution unstructured triangular meshes to capture the macro-roughness and modelled the 2011 Tohoku tsunami propagation in Kamaishi city, Japan. The unstructured mesh model offers great flexibility to model macro-roughness with various sizes and shapes, however, it also requires tremendous time and effort to construct the model meshes. On the other hand, structured mesh models require substantially less effort to construct and can be more computationally efficient. However, applying a high spatial resolution over the entire model domain can negate these gains.

In this study, a quadtree mesh was adapted in TUFLOW's HPC 2D Shallow Water Equation (SWE) solver to vary the spatial resolution according to the resolution of obstructions without significantly increasing the model mesh number in the entire calculation domain. A 'Sub-Grid-Sampling' approach (Kitts at el. 2020) was also adopted to consider the impact of the obstructions that are not mesh aligned. Model benchmark testing was carried out against a 1:50 scale flume experiment of the town of Seaside, Oregon (Park et al. 2013).

2. NUMERICAL MODEL

2.1 Numerical Solver

TUFLOW's HPC 2D Shallow Water Equation (SWE) solver (Collecutt and Syme, 2017) was adapted to support quadtree meshes. The solver uses an explicit 4th order in time and 2nd order in space Runge-Kutta finite volume TVD scheme to track cell averaged depth and velocity and is parallelised for CPU or GPU acceleration. The model mesh is refined using the quadtree method as illustrated in Figure 1. A cell can be refined by quarters and the refinement can be applied at multiple levels. The volume fluxes across each face are computed using the face normal velocities, the water depth at the face, and the relevant face width:

$$A_c \frac{\partial h_c}{\partial t} = \sum \phi_i + S_Q \tag{1}$$

$$\phi_1 = \Delta y u_1 h_1;\ \phi_3 = \Delta x v_3 h_3;\ \phi_4 = \Delta x v_4 h_4$$

$$\phi_{2,1} = \frac{\Delta y}{2} u_{2,1} h_{2,1};\ \phi_{2,2} = \frac{\Delta y}{2} u_{2,2} h_{2,2} \tag{2}$$

where A_c is the cell area, h_c is the water depth at the cell centre, S_Q is any volume source or sink, ϕ_i, u_i, v_i, h_i are flux, velocities and water depth at cell faces, respectively, and Δx and Δy are local cell widths.

The momentum flux in x and y directions (hu and hv) are stored and calculated at cell faces in a similar manner (Collecutt and Syme, 2017). For a quadtree mesh, if a face locates between cells with different sizes, the control volume for momentum calculation uses a rectangle as illustrated in Figure 1 (b).

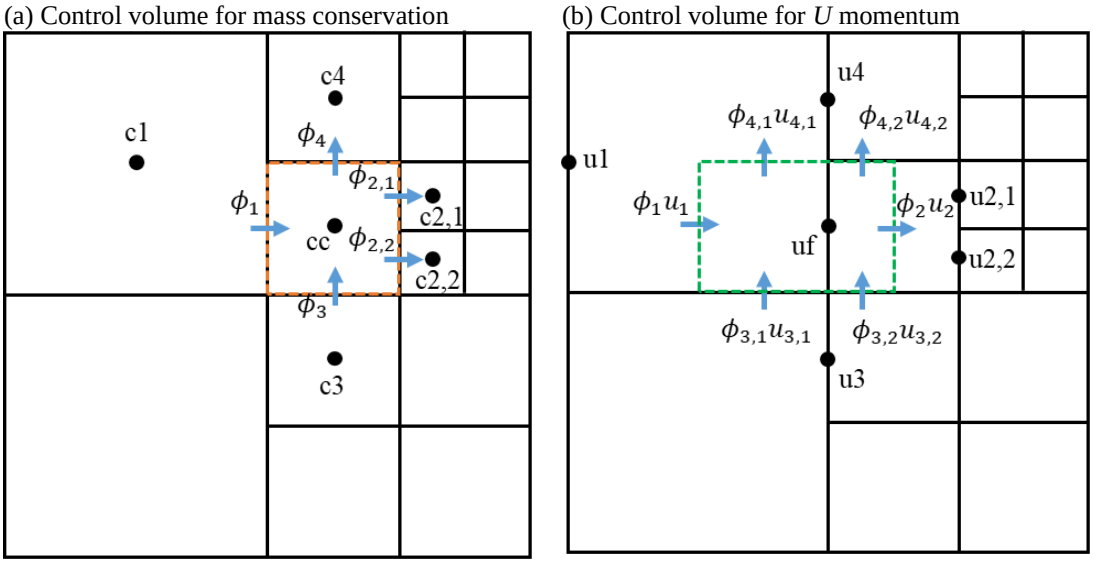

Figure 1. Control volume and fluxes for quadtree mesh.

Turbulent viscosity was assumed to be proportional to the friction velocity and the turbulence length scale is set to the minimum of water depth, or horizontal distance to the nearest dry boundary. The detail of the turbulence model benchmarking is discussed by Collecutt et al. (2020).

2.2 Sub-Grid Sampling

A 'Sub-Grid Sampling' (SGS) approach (Kitts et al. 2020) was adopted to consider the impact of macro-roughness that are not mesh aligned. This method samples the sub-grid scale topography for each cell and face to build non-linear relationships, in the case of cells, between the cell water volume and the water surface elevation, and in the case of faces, between the water surface elevation and the face flux area. This method essentially creates partially wet cells and faces along dry/wet boundaries, and may produce the same quality of results as a flexible mesh model or a cut-cell model. The impact of this method will be further discussed in the results section.

2.3 Modelling Condition

The flume experiment used for model verification was originally carried out by Rueben et al. (2011) and Park et al. (2013). A 1:50 scale physical model was constructed for the coastal town of Seaside, Oregon, USA. Rigid solid objects were placed to represent large hotels, commercial buildings, and residential houses (macro-roughness). Lidar-surveyed topography data has been provided by the author Dr. Hyoungsu Park for the modelling, allowing a 0.5 cm digital elevation model (DEM) to be constructed. The final topography used for the model domain is shown in Figure 2. The flume surface was smooth concrete with a flat finish, and a Manning's n of 0.011 was used in this study, based on the model calibration of the tsunami propagation at the

control section with no macro-roughness (the area below the divider wall in Figure 2). The initial water level was set as 0.97 m as per the experiment, and the inlet wave shape was calibrated to fit the measured water level at measurement point WG1. The modelling results are compared against the water levels recorded at other measurement points as illustrated in Figure 2. The mesh sizes of 5cm/10cm were applied in the onshore urban area and were extended to 10cm/20cm in the offshore section. The model was able to be comfortably solved on a mid-range laptop with Intel CPU i7-7500U (2.7GHz) and Nvidia GPU GeForce 940MX (384 CUDA cores).

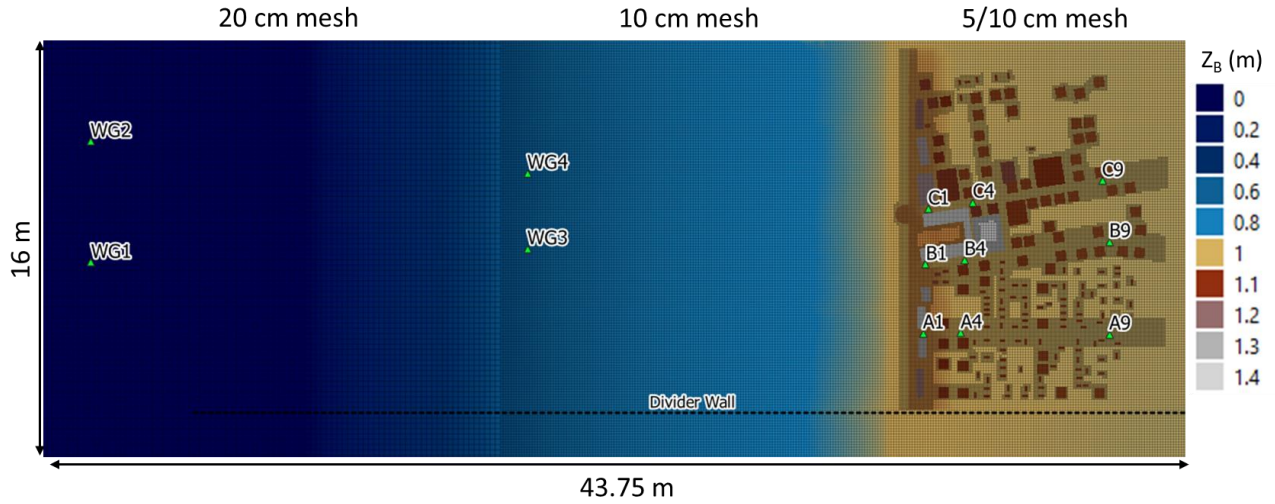

Figure 2. Modelling topography and measurement locations.

3. SIMULATION RESULTS

3.1 Tsunami Propagation

Figure 3 (a) presents the simulation results of water depth contour at t = 28.7s compared with the optical record of mean wave edge position (blue dashed line) over 21 experiment runs (Rueben et al., 2011). The simulation reproduced the tsunami wave overtopping of the short buildings and propagating through the streets. The wave propagated faster through the streets and slower over the block with dense macro-roughness, emphasizing the importance of high-resolution modelling in tsunami hazard planning. Section A1-A9 has relatively small buildings perfectly aligned with the computational mesh and the inundation area of the quadtree model (left) agreed well with the recorded edge position. However, Sections B1-B9 and C1-C9 have large buildings not well aligned with the computational mesh, and it is this region that benefits with the sub-grid sampling approach.

(a) Quadtree model (b) Quadtree model + SGS

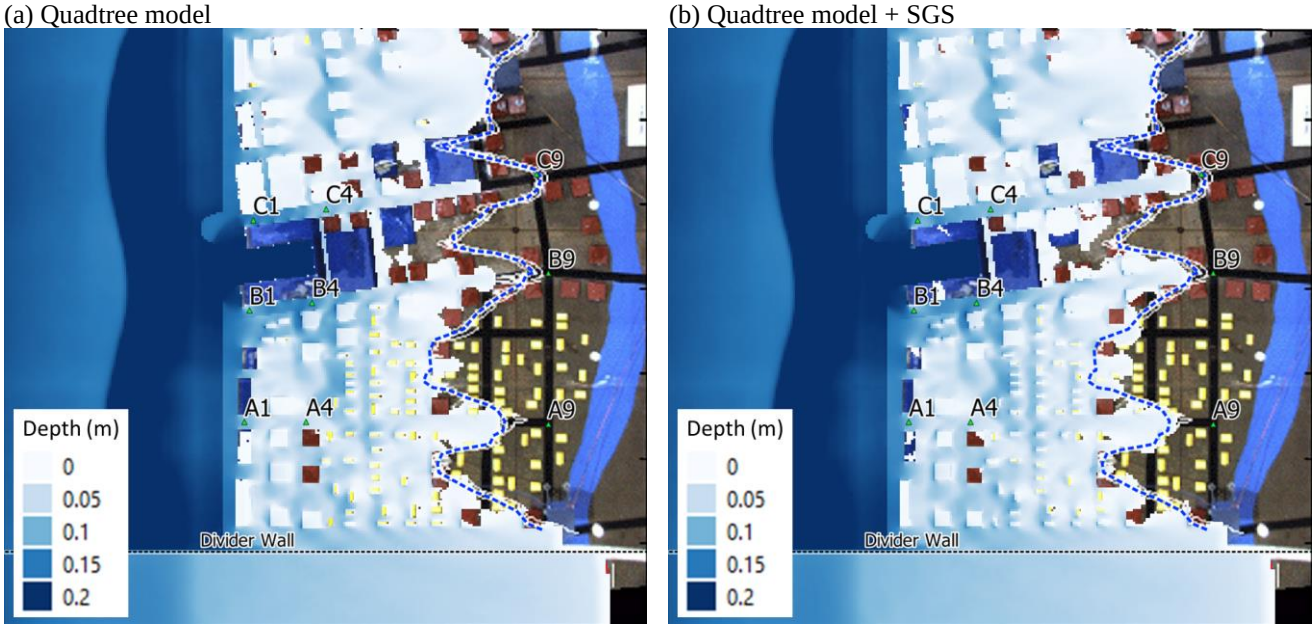

Figure 3. Comparison of tsunami wave front location at t = 28.7s. Blue dashed line highlights the recorded wave front location. By using SGS a much improved tidal wave propagation is evident as shown in the right image.

Figure 4 shows the modelled velocity vector and velocity magnitude contours near monitoring location C1, north to the largest U-shaped building. Without sub-grid sampling (Figure 4 (a)), some structured mesh

elements next to the building formed vertical walls against the direction of the flow and reduced the local velocity. This produced non-uniform (zig-zag) streamlines along the edge of the building resulting in artificial head losses and the shorter propagation distance.

The possibility of mitigating the artificial loss was investigated by (1) further refining the local mesh size, and (2) applying the SGS method, applied separately and together with the mesh refinement. Figure 4 (a) displays the original velocity field while Figure 4 (c) shows the same with additional mesh refinement (2.5cm mesh) along the edges of the buildings. However, the artefacts in the local velocity field are still visible. Figure 4 (b) and (d) present the same results respectively with the SGS approach included. Extra cells have been activated along the dry/wet boundary as partially wet cells. Even without the 2.5cm refinement, the velocity field along the edge of the building was smoother and the simulated tsunami wave propagated further onshore (Figure 3 (b)), which yielded a much improved agreement with the recorded wave position.

(a) Quadtree model, 20/10/5cm mesh

(b) Quadtree model + SGS, 20/10/5cm mesh

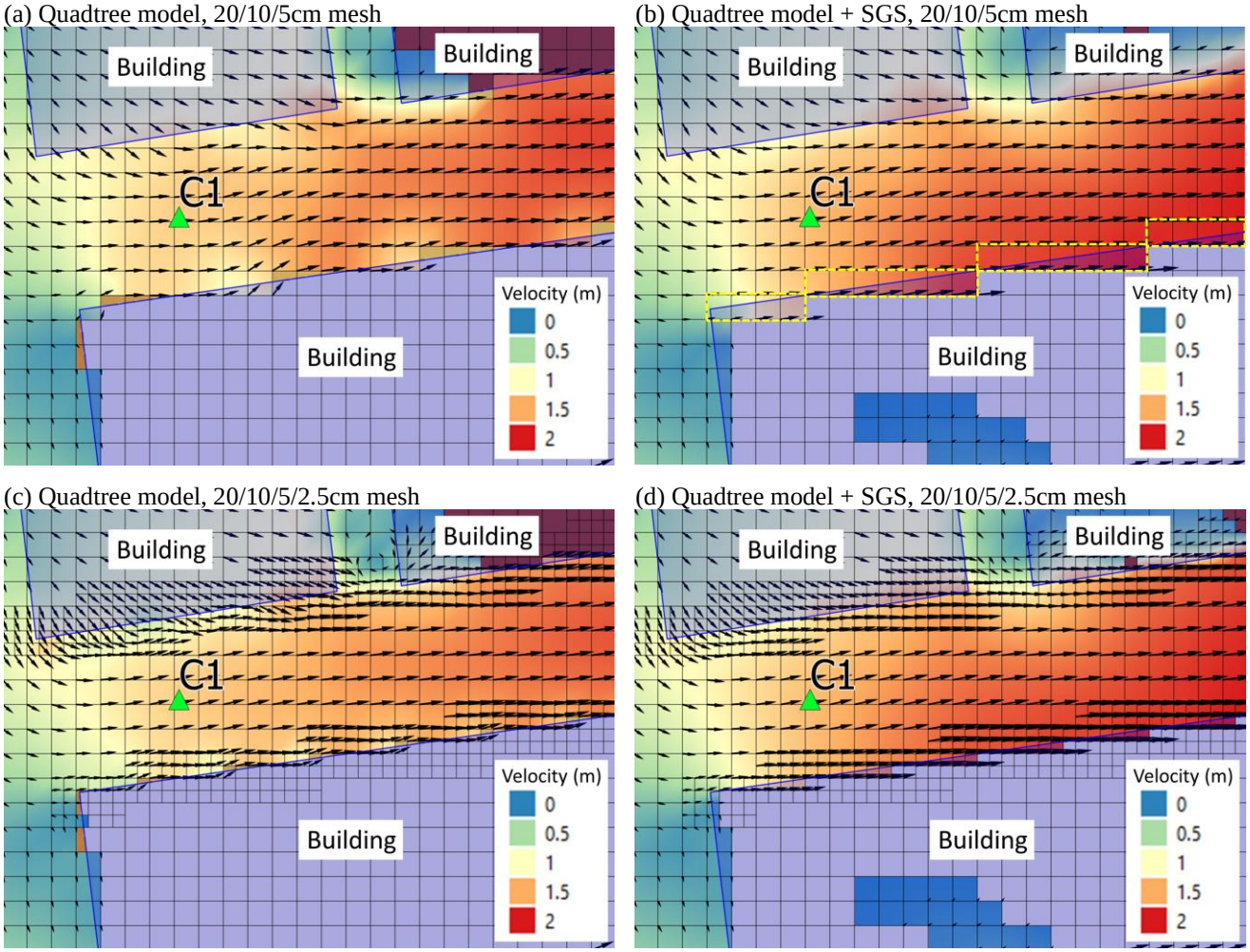

(c) Quadtree model, 20/10/5/2.5cm mesh

(d) Quadtree model + SGS, 20/10/5/2.5cm mesh

Figure 4. Velocity vector and velocity magnitude contours at location with obstacles not aligned with computational mesh. The non-uniform velocity patterns along the edge of the building are evident without SGS (left images), whilst entirely removed with SGS (right images).

Figure 5 compares the modelled and recorded water level increment at location A1, A4, A9 and C1, C4, C9. At Section A1-A9 (mesh aligned), the SGS and the non-SGS model produced similar results and generally agreed with the measured data. Both models under predicted the maximum water level surge at location A1. This monitoring point is located between the first rows of tall buildings, where the obstacles form a bottle neck for the propagating tsunami wave. The modelled and recorded results both show a rapid drop in maximum water level along the first few monitoring points. For example, shifting the simulation sampling location by one cell (5cm) to the ocean side may change the peak level by 0.015m. It is also interesting to note that location A9 recorded a second surge due to the reflection wave from the wall at the east of the experiment basin. This surge was better modelled by the SGS model, whereas it lagged in the non-SGS model.

At Section C1-C9, where there is mesh misalignment with the buildings, the SGS and the non-SGS model produced similar arrival time at location C1 and C4, but the SGS result predicted a better arrival time at location C9, which is consistent with the inundation contour map in Figure 3.

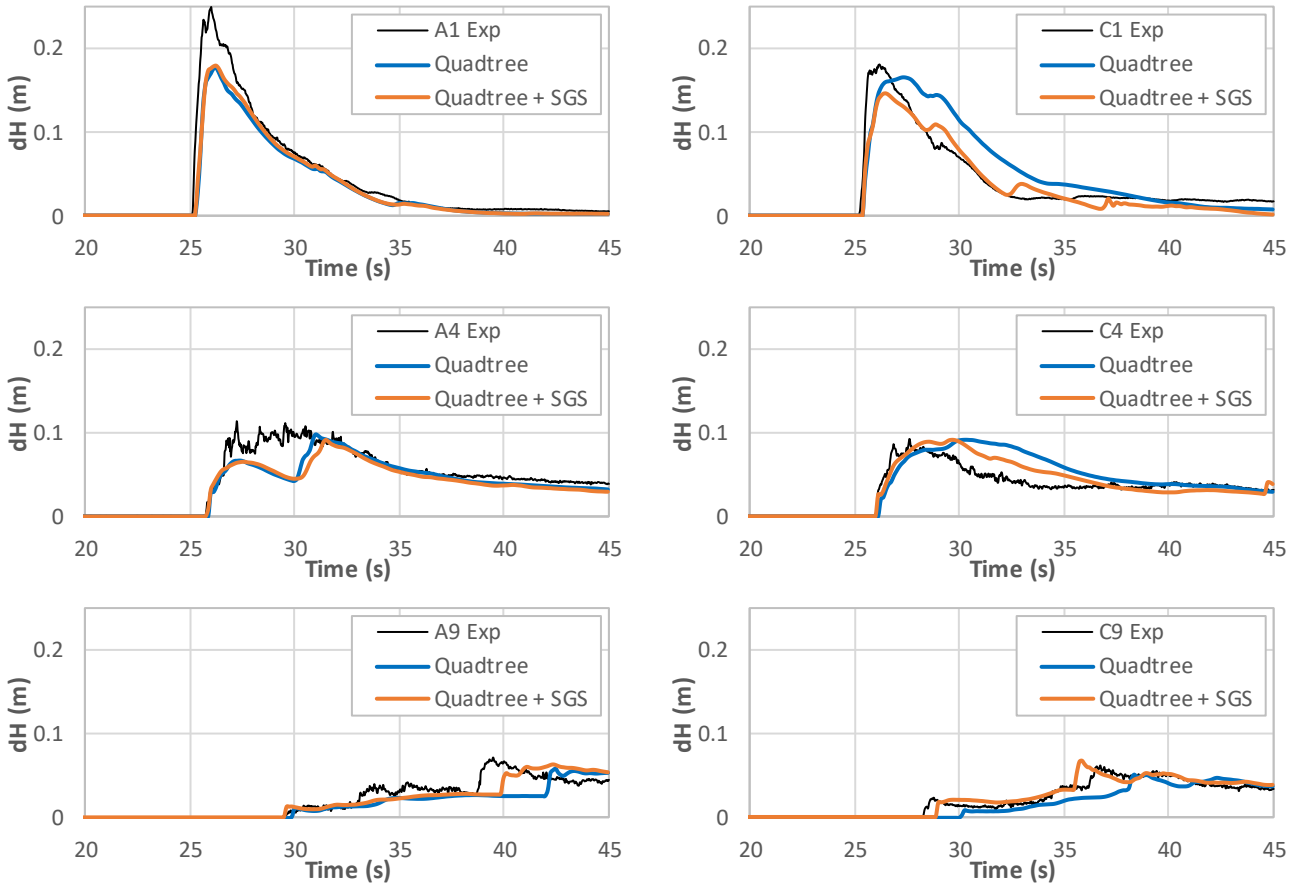

Figure 5. Time series of water level increase at monitoring location A1, A4, A9 and C1, C4, C9.

3.2 Computational times

Table 1 compares the number of cells and solution times between the quadtree models and a gridded model that uses a uniform mesh size of 5cm for the entire model domain. In this study the number of mesh cells was reduced by 75% using a quadtree approach along with simulation times that were 4.3 times faster. Although the quadtree solution scheme is slightly more complex, by using larger cells in the deep water regions the wave celerity constraint on the computational timestep was not as significant. As the SGS model conducts extra conversions between the water surface elevation and the cell volume and face flux area, the simulation speed is slightly slower than the non-SGS model. However, the benefit of eliminating the mesh alignment dependency in such type of urban environment almost certainly outweighs the time cost.

Table 1. Computational summary.

	Uniform grid	Quadtree Model	Quadtree + SGS
Cell Size (cm)	5	20/10/5	20/10/5
Number of Cells	284,796	72,492	72,492
Run Time (s)	358	83	111
Relative Speed up vs uniform grid model	-	4.3	3.2

4. CONCLUSIONS

This study utilised TUFLOW's HPC 2D solver quadtree feature to investigate modelling of tsunami inundation of coastal urban environments. The spatial mesh resolution was varied according to the resolution of macro-roughness to optimise the mesh structure. A 'Sub-Grid-Sampling' approach was also applied to mitigate the non-uniform streamlines and artificial head loss that occurs along cells that are not perfectly aligned with the flow obstructions. Model benchmark testing against the 1:50 scale flume experiment indicated:

1. By applying the quadtree refinement, the total number of the computational mesh elements was reduced by 75%, and the simulation speed was increased by 4.3 times.
2. Both SGS and non-SGS models showed good agreement with the measured results along Section A1-A9, where the macro-roughness is well aligned with the computational mesh.

3. The SGS model substantially improved the modelling results along Section B1-B9 and C1-C9, where the macro-roughness is not aligned with the computational mesh. The improvement achieved by selecting the SGS approach was more significant than that achieved through halving the local mesh size in a non-SGS model.
4. The combination of quadtree mesh and SGS approach offers great potential as an easy to construct, fast, accurate, high-resolution numerical tool to support tsunami hazard planning.

ACKNOWLEDGMENTS

We thank Dr. Hyoungsu Park from University of Hawai and Professor Daniel T. Cox from Oregon State University for kindly sharing the topography and measurement data.

REFERENCES

Rueben, M., Holman, R., Cox, D., Shin, S., Killian, J., Stanley, J. (2011) Optical measurements of tsunami inundation through an urban waterfront modeled in a large-scale laboratory basin. *Coastal Engineering*, 58:229–238.

Park, H., Cox, T. D., Lynett, P. J., Wiebe, D. M., and Shin, S. (2013) Tsunami inundation modeling in constructed environments: A physical and numerical comparison of free-surface elevation, velocity, and momentum flux. *Coastal Engineering*, 79:9–21.

Akoh, R., Ishikawa, T., Kojima, T., Tomaru, M., and Maeno, S. (2017). High-resolution modeling of tsunami run-up flooding: a case study of flooding in Kamaishi city, Japan, induced by the 2011 Tohoku tsunami. *Natural Hazards and Earth System Science*. 17:1871–1883.

Kitts, D., Syme, W., Gao, S., Collecutt, G., Ryan, P. (2020). Mesh Orientation and Cell Size Sensitivity in 2D SWE Solvers. Submitted paper for the *IAHR 10th Conference on Fluvial Hydraulics*, River Flow 2020, Delft, Netherlands.

Collecutt, G., and Syme, B. (2017). Experimental benchmarking of mesh size and time-step convergence for a 1st and 2nd order SWE finite volume scheme. *Proceedings of the 37th IAHR World Congress*, Kuala Lumpur.

Collecutt, G., Gao, S., and Syme, W.J. (2020). Turbulence Modelling for the 2D Shallow Water Equations. Submitted paper for the *IAHR 10th Conference on Fluvial Hydraulics*, River Flow 2020, Delft, Netherlands.